Stealth fluorescence labeling for live microscopy imaging of mRNA delivery

Tom Baladi, Jesper R. Nilsson, Audrey Gallud, Emanuele Celauro, Cécile Gasse, Fabienne Levi-Acobas, Ivo Sarac, Marcel Hollenstein, Anders Dahlén, Elin K. Esbjörner, et al.

Stealth fluorescence labeling for live microscopy imaging of mRNA delivery

Tom Baladi,[a,b]† Jesper R. Nilsson,[a] Audrey Gallud,[c]‡ Emanuele Celauro,[c] Cécile Gasse,[d] Fabienne Levi-Acobas,[e] Ivo Sarac,[e] Marcel Hollenstein,[e] Anders Dahlén,[b]† Elin K. Esbjörner*[c] and L. Marcus Wilhelmsson*[a]

a Department of Chemistry and Chemical Engineering, Chemistry and Biochemistry, Chalmers University of Technology, SE-41296, Gothenburg, Sweden.

b Medicinal Chemistry, Research and Early Development, Cardiovascular, Renal and Metabolism, BioPharmaceuticals R&D, AstraZeneca, Gothenburg, Sweden.

c Department of Biology and Biological Engineering, Chemical Biology, Chalmers University of Technology, SE-41296, Gothenburg, Sweden.

d Génomique Métabolique, Genoscope, Institut François Jacob, CEA, CNRS, Univ Evry, Université Paris-Saclay, 91057 Evry, France.

e Institut Pasteur, Department of Structural Biology and Chemistry, Laboratory for Bioorganic Chemistry of Nucleic Acids, CNRS UMR3523, 28, rue du Docteur Roux, 75724 Paris CEDEX 15, France

KEYWORDS modified nucleobase triphosphate, fluorescence labeling, mRNA, translation, live cell imaging, drug delivery

ABSTRACT: Methods for tracking RNA molecules inside living cells without perturbing their natural interactions and functions are critical within biology and, in particular, to facilitate studies of therapeutic RNA delivery. We present a stealth labeling approach that can efficiently, and with high fidelity, generate RNA transcripts of any length, through enzymatic incorporation of the triphosphate of tC^O – a fluorescent tricyclic cytosine analogue. We demonstrate this by incorporation of tC^O in up to 100% of the natural cytosine positions of a 1.2 kb mRNA encoding for the histone H2B fused to GFP (H2B:GFP). Spectroscopic characterization of this mRNA shows that the incorporation rate of tC^O is similar to cytosine, which not only indicates tC^O's excellent nucleotide analogue properties, but also the possibility for efficient labeling and controlled tuning of labeling ratios for different applications. Using live cell confocal microscopy and flow cytometry, we show that the tC^O-labeled mRNA is efficiently and correctly translated into H2B:GFP inside human cells. Hence, we not only pioneer the use of fluorescent base analogue labeling of nucleic acids in live-cell microscopy but also, importantly, show that the resulting transcript can be correctly translated. Moreover, the spectral properties of our transcripts and their translation product allow for their straightforward, simultaneous visualization in live cells. Finally, we find that transfected tC^O-labeled RNA, unlike the corresponding state-of-the-art fluorescently labeled RNA, translates equally efficient as its natural counterpart, hence representing a methodology for studying natural, unperturbed processing of mRNA used in RNA therapeutics as well as in vaccines, like the ones currently under development against SARS-CoV-2.

INTRODUCTION

RNA is a key molecule of life and a main active player of the central dogma of molecular biology. RNA is also a crucial regulator of gene expression via for instance micro (mi)- and small interfering (si)-RNA and through its intrinsic catalytic activity; RNA therefore plays a fundamental role in biology. It has, for these reasons, emerged as a highly promising and versatile drug modality with potential to modify cellular function at the translational level opening up entirely new avenues to address previously undruggable targets.[1] Increased molecular and mechanistic knowledge of biological processes that involve RNA is therefore important and requires, in many instances, new methodological tools. In the context of RNA therapeutics, cellular delivery remains a major challenge and better understanding of cellular uptake, endosomal release, and cytosolic delivery of RNAs is needed to unleash their full potential.[2-4] A major problem in this regard relates to the challenge of directly visualizing RNA molecules as they are taken up, processed, and subsequently released into the cytosol.[5]

Recent advances in RNA imaging have generated a broad spectrum of tools and probes by which RNA can be analyzed and quantified, but they generally rely on the use of heavily modified externally labeled oligonucleotides with chemical and physical properties that are significantly different from their natural counterparts. Cyanine dyes

such as Cy3 and Cy5 conjugated for instance via strain-promoted cycloaddition linkers remain the most common labeling choice,[6-7] even though their bulkiness and hydrophobicity significantly impede both transcription and translation[8] (has also been noted by TriLink Biotechnologies, one of the main manufacturers of externally labeled mRNA) of mRNA. Development of more universally applicable RNA labeling schemes and probes that are minimally perturbing to RNA's functions, and compatible with live-cell fluorescence imaging is therefore needed and may become as crucial for the RNA field as the discovery and understanding of the green fluorescent protein (GFP) has been for proteins.[9-11]

A major challenge in RNA imaging is to develop new methods and probes that are functional in living cells.[12] While methods reliant on cell fixation such as fluorescence in situ hybridization (FISH) can visualize and quantify mRNA interactions with astounding specificity and single molecule resolution,[13] they fall short with respect to capturing the spatiotemporal and conformational dynamics that are important to RNA function. The development of FRET-pair functionalized antisense oligonucleotides (ASOs)[14-15] is highly interesting in this regard, but requires binding of at least two ASOs to the mRNA target, which may sterically block protein binding sites, hinder mRNA translation or induce tertiary structure formation; in practice the method has also mainly been used on fixed cells. To visualize RNA in live cells, probes are often conjugated to a vehicle, such as a DNA nanocages,[16] or gold nanoparticles,[17] before delivery. Another emerging strategy is to fuse the RNA of interest to an aptamer sequence that binds fluorescent dyes in situ,[18] but this can also adversely influence translation efficiency and RNA-protein interactions.[19] To reduce the risks of interfering with enzymatic processes, chimeric mRNAs have been developed with multiple stem-loop structures downstream of the STOP codon, which serve as binding sites for fluorescent fusion proteins.[20,21-22] Whilst versatile, all these labeling strategies impact profoundly on the physicochemical properties and molecular weights of RNAs and therefore risk to significantly perturb their natural function, spatiotemporal distribution and transport.

Additional less perturbing strategies for labeling mRNA have therefore been developed, relying for example on click chemistry approaches with azido-functionalized 5′-cap analogues[23], 3′-polyA tails,[24] or nucleotides[25] enabling in cell post-transcriptional labeling of mRNA. Similarly, Ziemniak et al., have produced a range of fluorescent 5′-cap analogues that are compatible with both transcription and translation;[26] However, the resulting mRNA products only carry one single label and have therefore not been possible to visualize inside cells, limiting the applicability of this method.

Fluorescent nucleobase analogues (FBAs) have emerged as attractive labels for DNA and RNA. However, even though we and others have significantly improved FBAs with respect to brightness, excitation and emission to facilitate their use in fluorescence microscopy,[27-29] significant challenges have remained regarding development of FBAs that are sufficiently enzyme-compatible to be effectively processed during transcription and translation.[30] FBAs have the advantage of being internal fluorophores, with relatively small chemical modifications to the natural base which they replace. Furthermore, their design enables normal base-pairing and -stacking of the target nucleic acid. FBAs are therefore considered to be native-like fluorescent labels and have been extensively used in vitro to probe nucleic acid structure and behavior. We have, for example, designed FBA interbase FRET-pairs to obtain detailed information on the structure and base orientation in DNA[31] and RNA [32,33] and others have used FBAs to study biophysically ribosome-mediated codon:anticodon base-pair formations.[34] A handful studies indicate that FBAs can be incorporated into RNA via cell-free transcription resulting in for example ca. 800 nucleotide (nt) RNA strands with a modified cystosine[35] or short transcripts with fluorescent isomorphic guanine[36-37] and uridine.[38-39] However, none of these studies have proven that FBA transcripts can be translated and FBA-labeled RNAs have not yet been used in biological applications or to visualize RNA molecules inside of living cells. This progress is needed to translate FBAs from useful in vitro probes to functional tools for chemical and medical biology.[30]

In this study, we demonstrate that the fluorescent tricyclic cytosine analogue 1,3-diaza-2-oxophenoxazine (tC^O; Abs_{max}=369 nm; Em_{max}= 457 nm; ε_{369} = 9370 M^{-1} cm^{-1}; $<\Phi_F>$ = 0.24)[32] can be enzymatically incorporated in high numbers into RNA via end-labeling reactions as well as cell-free transcription. We furthermore show that it is possible to exchange all natural cytosines in a 1.2 kb long mRNA for tC^O (Figure 1) and retain translation competence both in vitro and in human cells. We also demonstrate, for the first time, that an FBA-labeled mRNA can be sufficiently fluorescent to be directly visualized by confocal microscopy in a living human cell and used to study mRNA delivery and protein translation in a drug delivery context.

This presents a significant advance to the FBA and RNA imaging fields and a new powerful tool to enable effective visualization of RNA and thereby enable studies of RNA function, trafficking, and localization in a variety of cellular contexts, including for example drug delivery, virus processing, and exosome biology.

RESULTS AND DISCUSSION

Synthesis of the tricyclic cytosine analogue (tC^O) triphosphate. The tC^O ribonucleotide has, unlike the corresponding nucleoside, never been synthesized and, hence, we needed to establish a synthetic route towards our target molecule. Since the Yoshikawa[40] and Ludwig-Eckstein[41] conditions were published in 1969 and 1989, respectively, a plethora of methods have been proposed for the triphosphorylation of nucleosides,[42-45] but no generic method exists to effectively synthesize and purify ribonucleotides in the high yields that are required for practical use in biochemical applications.

To overcome this "hit-and-miss" aspect of ribonucleotide synthesis, we developed a new synthesis scheme that requires no preliminary protection of the 2'- and 3'-positions and that facilitates purification of the final product (Figure 1). In our hands, this new method allowed the synthesis of the tC^O nucleotide used herein and two additional nucleobase-modified nucleotides (manuscripts in preparation) in equally good yields and we envision it could there-

fore become a generic and convenient route towards any modified nucleotide.

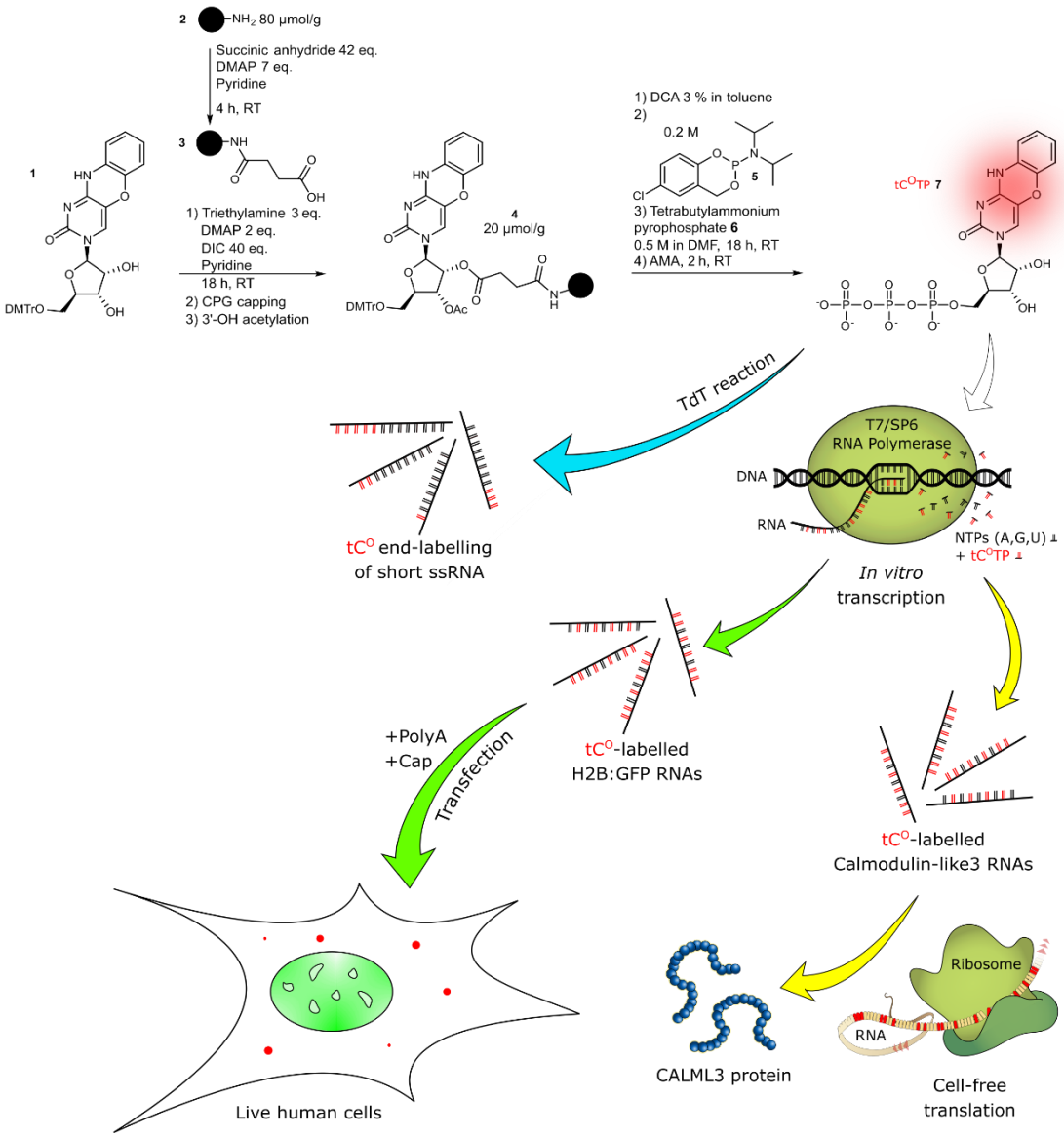

Figure 1. Schematic outline of the study with the synthesis of main building-block of the study, the fluorescent tricyclic cytosine analogue tC^O triphosphate **7**, at the top. **Blue pathway**: End-labeling of ssRNA sequences using a terminal deoxynucleotidyl transferase (TdT). **Green pathway**: Cell-free transcription into H2B:GFP mRNA, transfection into human cells and live-cell imaging of both the GFP protein (translation product) and tC^O (mRNA). **Yellow pathway**: Cell-free transcription into Calmodulin-like3 RNA followed by cell-free translation into the CALML3 protein. Color code: tC^O in red, GFP in green, native nucleosides in black or beige.

The tC^O ribonucleotide was synthesized from a solid-supported ribonucleoside; a strategy that has never been reported for modified nucleobases, but attempted with some success for unmodified nucleobases with 2′-OMe backbone protection. Our synthetic scheme relies on phosphoramidite chemistry, which involves the use of *Cyclo*Sal-phosphoramidite **5** and bis(tetrabutylammonium) dihydrogen pyrophosphate **6** (Figure 1). This approach was developed by Meier et al.[46] to achieve efficient 5′-triphosphorylation of short solid support-bound DNA and RNA oligonucleotides in moderate to good yields. In our hands, both Krupp's[47] and Meier's[46] solid-phase triphosphorylation methods yielded the product, though Meier's gave a higher yield. To the best of our knowledge, the *Cyclo*Sal-phosphoramidite method on solid support described herein has never been applied to a single ribonucleoside before, let alone to produce a modified nucleotide.

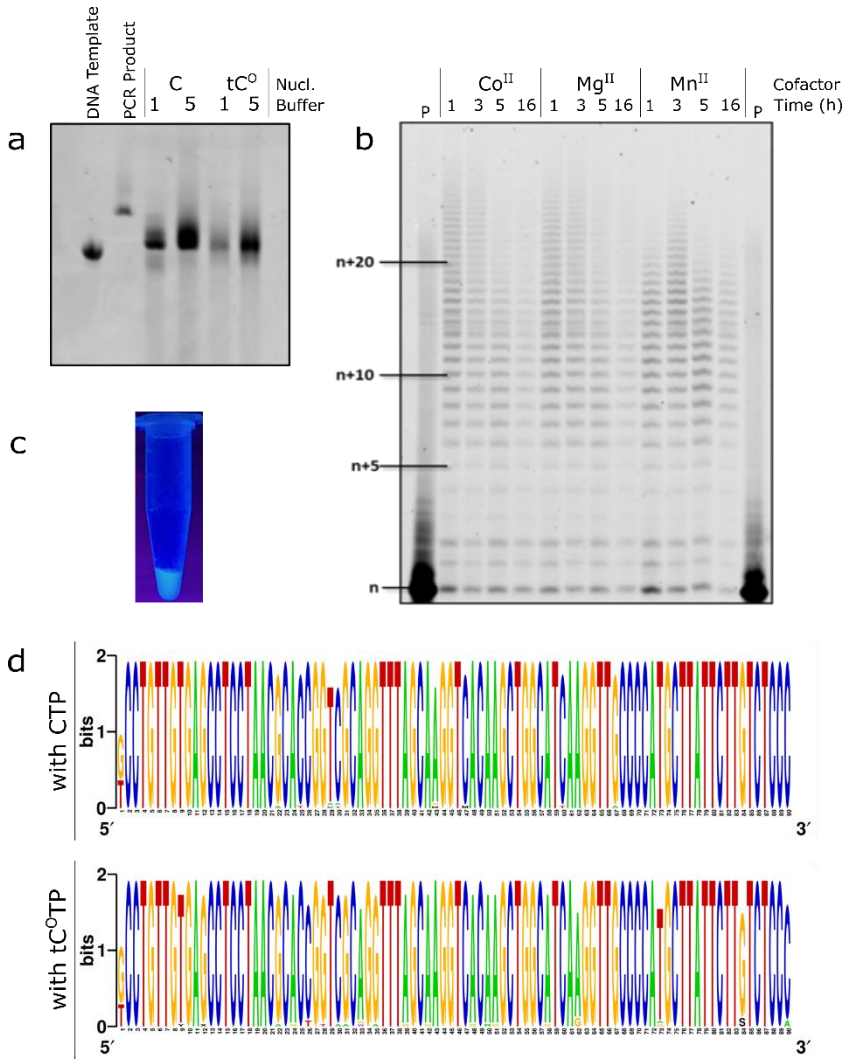

Figure 2. Enzymatic incorporation of the modified triphosphate by cell-free transcription on short templates, sequencing of reverse transcriptase products and TdT-mediated labeling. a) Gel image (PAGE 10%; visualization by midori green) of RNA products from 6 h of T7 RNA polymerase assisted transcription using the D1 Library as DNA template. See Methods for buffers composition. b) Gel image (PAGE 20%; visualization by phosphorimager) of the products from TdT-mediated end-labeling of oligonucleotide TdT1 using tC^{O}TP. The lowest band labeled "n" represents the unreacted TdT1 oligonucleotide and all above bands are different products with increasing additions of tC^{O} to the tail. P: control reaction in absence of polymerase. c) Picture of UV-light irradiated solution of purified TdT3 RNA end-labeled with tC^{O}. d) Sequence logo from the cloning-sequencing protocol of reverse transcription products from the modified T12.3 RNA (top: products from a 6 h transcription reaction with CTP; bottom: products from a 6 h transcription reaction with tC^{O}TP). Lower (stars) and higher (arrow) frequency A to G transversions are highlighted.

Briefly, long-chain alkylamino controlled-porosity glass (CPG) support was functionalized with a succinyl moiety. Protected ribonucleoside **1** was synthesized according to a method by Füchtbauer et al.[32] and attached to the succinylated support via ester bond formation (Figure 1). The resulting ribonucleoside **4** on solid support could be stored in the dark at room temperature, with no degradation observed over three months. Interestingly, intermediate **4** could also be synthesized via succinylation of ribonucleoside **1** in solution followed by coupling with the amino support **2**. In both cases, the starting nucleoside could be used unprotected at the 2'- and 3'-positions, thus eluding the need for additional protection steps, which makes our method straightforward. Subsequently, triphosphorylation of ribonucleoside **4** was performed using the *Cyclo*Sal method. After triphosphorylation, support-bound triphosphate was deacetylated and cleaved from the CPG support using ammonium hydroxide/methylamine (AMA) for two hours at room temperature. Subsequent reverse phase or ion-exchange chromatography allowed the desired triphosphate **7** in a triphosphorylation yield of 60% and with a high UV purity of 99%. Importantly, up to 85% of the unreacted nucleoside **1** could conveniently be recovered by precipitation from the first reaction crude, compensating for the low loading achieved. Considering this, our triphosphorylation method gives an overall yield of up to 30%, of the tC^{O} ribonucleotide which is higher than most solution-based alternatives.

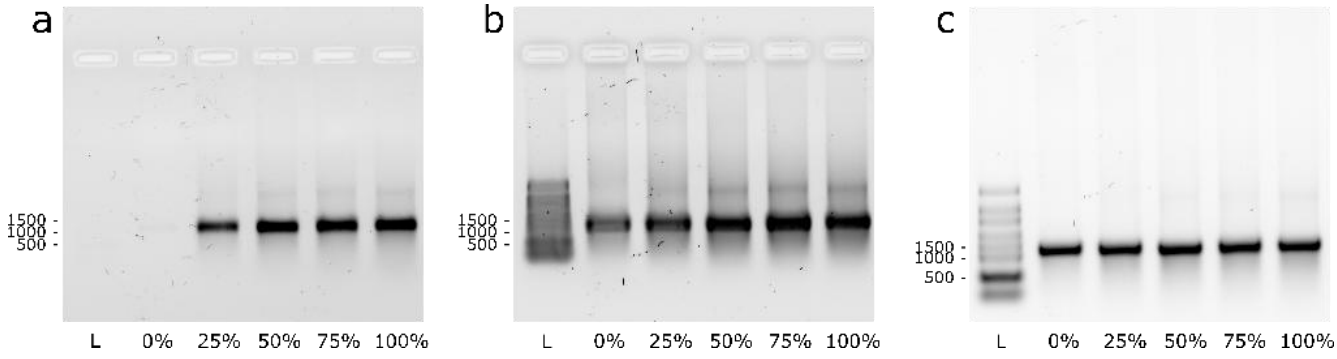

Figure 3. Incorporation of tC^O into full length mRNA by T7 RNA polymerase assisted cell-free transcription. Denaturing agarose bleach gels showing RNA transcripts formed at five different tC^{O}TP/CTP ratios (0-100%). Direct visualization of tC^O fluorescence (a) and after ethidium bromide staining (b). RNA samples were heat-denatured (65 °C for 5 min, 1.5% bleach in the gel) prior to loading. (c) Same RNA transcripts upon harsher denaturation (70 °C for 10 min., 2% bleach in the gel). The RiboRuler High Range RNA ladder was used.

Cell-free enzymatic incorporation of tC^O into RNA. The tC^O ribonucleotide (tC^{O}TP) was used to produce fluorescently labeled RNA via two different enzymatic methods.

First, we tail-labeled short RNA oligonucleotides using the terminal deoxynucleotidyl transferase enzyme (TdT, Figure 1, blue arrow), which catalyzes template-independent addition of random nucleotides to 3'-overhangs in both DNA and RNA.[48-49] Starting from a 17-mer ssRNA (TdT1, see Supplementary Table 1 for sequence) we demonstrate successful addition of multiple adjacent tC^{O}s (from one to > 25) on nearly all RNA primers (Figure 2b). The addition was equally effective with Co(II), Mg(II), or Mn(II) as co-factor in accord with the normally reported function of TdT,[48] supporting a native-like enzymatic processing of tC^O, which was confirmed also in our case, with equally effective addition of tC^{O}s with the corresponding enzymatic co-factors. TdT-mediated tail-labeling of longer (50 nt, TdT2, Supplementary Table 1) ssRNA sequences was also successful and the main products were more uniform, containing typically one or two tC^O (Supplementary Figure 1). The lower processivity found for this longer RNA could be an effect of its length or of its 3'-sequence but more likely due to the fact that the TdT is a DNA polymerase that prefers deoxyribonucleotides both as substrates and as templates. The fluorescence originating from a tC^O tail-labeled RNA was clearly observable by naked eye upon UV irradiation (Figure 2c). This proves that it is possible to use tC^O to site-specifically end-label RNA of any length, which represents an advantage in terms of enabling dual labeling of RNA strands, where combinations of tC^O with other base- or backbone-modified fluorescent markers will enable monitoring of for example in vivo stability.

We also tested the capacity of T7 RNA polymerase to incorporate tC^{O}TP into short (20 nt/90 nt; Supplementary Table 1) RNA transcripts, observing successful transcription without premature transcription termination even upon complete replacement of canonical CTP with tC^{O}TP (Figure 2a, Supplementary Figure 2a, and Supplementary Figure 3). This confirms that tC^{O}TP is readily accepted also by the T7 polymerase as a substrate. To further assess the enzymatic processing of tC^{O}TP, we tested its propensity to be misinserted opposite to a single deoxyadenosine downstream of the T7 promotor sequence of a guanosine-free DNA template (Supplementary Table 1; DNA3, DNA4). Transcription reactions were run in the presence of either CTP or tC^{O}TP and absence of UTP (Supplementary Figure 2b). With the first template (DNA3), no noticeable difference was observed in the reactivity of tC^{O}TP and CTP, whereas a mismatch closer to the T7 promoter sequence (DNA4), resulted in slightly fewer aborted transcripts and hence more full-length transcripts with tC^{O}TP compared to native CTP. This suggests a minor (20% based on densiometric analysis, see Supporting information) increase in error frequency with tC^{O}TP. A previous report by Stengel et al. used a structurally related tricyclic cytosine analogue tC, which carries a bulkier sulfur atom instead of an oxygen at position 5 of the pyrimidone ring, to produce RNA transcripts. Their reaction proceeded with a considerable formation of mismatched tC-A base pairs (a discrimination factor of 40 against was reported).[35] As a further comparison to this we tested the fidelity of incorporation of tC^{O}TP by reverse transcription (Supplementary Figure 3). After PCR amplification and A-tailing reaction, the resulting amplicons were ligated to the pGEM T vector and transfected into beta 2033 competent E. coli cells and plasmids stemming from white colonies were subjected to Illumina sequencing. Multiple alignment analysis revealed a mere two-fold higher frequency of misincorporation with tC^{O}TP compared to CTP (28 vs. 16 points mutations in respectively 34 and 38 analyzed sequences; Supplementary Figure 4-6); significant A to G transversion was observed at position 62 (3 mutations, Figure 2d and Supplementary Figure 6). In combination with the above-mentioned minor difference in abortion frequency (20% or lower) found between CTP and tC^{O}TP, this suggests an overall lower level of misincorporation for tC^{O}TP than for the analogue reported by Stengel et al.. Altogether, this shows that the fluorescent tC^{O}TP nucleotide is well-tolerated by both TdT and T7 RNA polymerases, with the latter only marginally increasing the incorporation error rate in up to 50 nt long RNAs. In this sense, tC^{O}TP behaves better than a majority of previously modified nucleotides,[35-36, 50-52] including bulkier triphosphate analogues.[53-54] It has been reported that the T7 RNA polymerase binds the incoming nucleotide substrate in an open conformation,[55] which could enable it to accommodate our modified base.

Cell-free enzymatic incorporation of tC^O into full length mRNA transcript. We next extended the in vitro transcription to test if it was possible to produce full length, translationally active mRNAs with different degrees of tC^O.

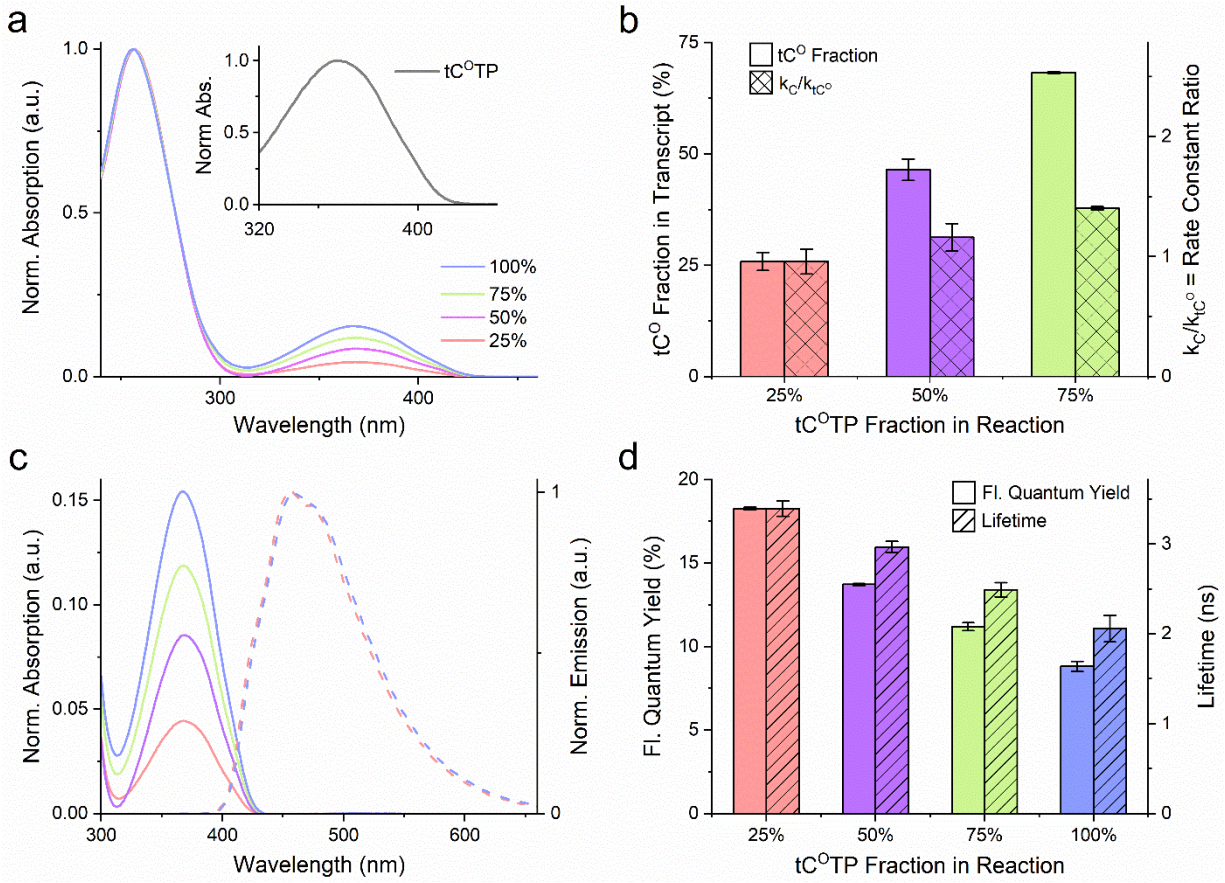

Figure 4. Spectroscopic characterization of cell-free synthesized tC^O-modified RNA transcripts. Four reactions charged with different molar fractions of tC^{O}TP (blue: 100%, green: 75%, magenta: 50%, and red: 25%) in the total cytosine triphosphate pool (tC^{O}TP + CTP) were performed. The product transcripts were purified to wash out unreacted triphosphates prior to characterization. All reactions were performed as independent duplicates and the results are presented as mean ± standard deviation. a) UV-vis absorption spectra normalized to A = 1 at the RNA band, ca. 260 nm. Inset: tC^{O}TP absorption normalized to A = 1 at the tC^O-band λ_{max} (360 nm). b) Plain bars: Fraction of incorporated tC^O (relative to the total amount of incorporated cytosines, i.e. tC^O + C) in the transcripts. Checkered bars: Ratio of first-order reaction rate constants for CTP vs. tC^{O}TP consumption. c) Solid lines: UV-vis absorption spectra (normalized to A = 1 at the RNA band, ca. 260 nm) showing the tC^O-band centered at 368–369 nm. Dashed lines: Emission spectra normalized to I = 1 at λ_{max} (457 nm and 459 nm for the 25% and 100% transcript, respectively). For clarity, the emission spectra for the 50% and 75% reactions were omitted. d) Plain bars: Fluorescence quantum yields. Striped bars: Fluorescence lifetime.

Transcription of long RNA containing a fluorescent base analogue has only been reported once,[35] but their ca. 800 nt transcript was not active in reverse transcription and no translation activity was reported, suggesting that the transcripts were non-functional. Moreover, they showed that increasing the amounts of their fluorescent tricyclic cytosine nucleotide the transcription reaction led to shorter transcripts, suggesting premature termination. Apart from being a fluorophore with superior brightness we envisioned that tC^O, with its oxygen in the middle ring instead of the considerably bulkier sulfur (vdW radius of sulfur is 20-30% larger resulting in an approximately 100% larger occupied volume) for the tricyclic cytosine used by Stengel et al, would represent a better cytosine analogue that would minimize perturbations to biological processes. We used a DNA template encoding for histone protein H2B fused to GFP (H2B:GFP) to produce mRNA via cell-free transcription. The template was codon optimized (Supplementary Figure 7) to limit the number of C repeats to limit self-quenching of adjacent tC^O moieties[56] (vide infra). We observed efficient transcription and tC^O incorporation with both T7 and SP6 RNA polymerases (Figure 1, first green arrow) at tC^{O}TP/canonical CTP ratios ranging from 0 to 100% (full replacement), as demonstrated by agarose bleach gel electrophoresis of the resulting transcripts (Figure 3a, Supplementary Figure 8a). The RNA transcripts appeared as one single band, with a migration corresponding to the expected 1247 nt mRNA product (H2B:GFP), demonstrating that full length mRNA was formed. The tC^O-containing mRNA bands could be directly visualized upon 302 nm excitation using a conventional gel scanner (Figure 3a); the increasing band intensities with increasing tC^{O}TP/CTP reaction ratio supported successful concentration-dependent incorporation of tC^O. Ethidium bromide

staining (Figure 3a, right) revealed similar amounts of RNA in all reactions, suggesting that tC^O incorporation does not reduce the cell-free transcription reaction yield. Furthermore, unlike the RNA product formation reported by Stengel et al.[35] no shorter transcripts were observed, strengthening the conclusion that the T7 RNA polymerase processes tC^OTP correctly and without premature abortion. Faint higher order bands were apparent with all tC^O-containing RNA transcripts (Figure 3b and Supplementary Figure 8b), but could be effectively removed by heat denaturation (Figure 3c), suggesting that the transcript has some propensity to induce RNA secondary structure. Notably, this feature appears independently of the CTP/tC^OTP-ratio but to various extents, indicating that it is not merely an effect that can be attributed the modified cytosine base. Importantly, we demonstrate that tC^O can be successfully incorporated into full-length mRNA and that this reaction proceeds effectively even when canonical CTP is completely replaced with tC^OTP, suggesting that this base analogue is highly mimetic of its natural counterpart.

Incorporation efficiency and spectroscopic properties of tC^O-containing mRNA. We used absorption and fluorescence spectroscopy to quantify the incorporation efficiency of tC^OTP compared to canonical CTP, following purification of the RNA transcripts using a commercial clean-up kit to remove unreacted tC^OTP. Absorption spectra (Figure 4a) of tC^O-containing transcripts shows an absorption peak at 370 nm, consistent with its reported spectrum inside RNA.[32] The relative magnitude of this peak compared to the RNA absorption at 260 nm (reflecting total concentration) confirms that the degree of tC^O incorporation is concentration-dependent, and allowed us to determine the relative rate constants for the incorporation of CTP and tC^OTP (k_C and k_{tCO}, respectively, see Methods for details). The ratio between the rate constants k_C/k_{tCO} were close to or slightly above unity for all transcripts (0.96–1.4, Figure 4b), suggesting strongly that T7 RNA polymerase discriminates only marginally between CTP and tC^OTP. Our observation of equal incorporation efficiencies for tC^OTP and CTP differs from other published studies where the corresponding incorporation ratio was found to be lower than 0.6 (and down to 0.13) for d(tC^OTP) incorporation into DNA, and analogues d(tCTP) into DNA and tCTP into RNA.[35, 57-58] This suggests that tC^O is a good nature-mimic with minimal perturbing effects on the transcriptional process. Furthermore, a trivial but noteworthy consequence of the determined rate constants, is that the tC^O incorporation degree in our mRNA matches extremely well the percentage of tC^OTP added to the transcription reaction (Figure 4b).

In quantitative fluorescence-based cell analyses, it is important that fluorescence intensity is proportional to probe concentration. We therefore examined the emissive behavior of tC^O in the mRNA transcripts as function of its degree of incorporation. We report a minor red-shift of the emission spectrum (ca. 4 nm) with increasing tC^O incorporation (Figure 4c) whereas more significant effects were observed on fluorescence quantum yields and lifetimes (Figure 4d). The figure shows that the quantum yield drops from 0.18 at 25% incorporation to 0.09 at 100% incorporation, consistent with a corresponding drop in fluorescence lifetime from 4.3 ns to 3.2 ns. We ascribe this to electronic coupling of molecular states of the tC^O fluorophore and a self-quenching effect[56] due to increased adjacency between tC^Os[57] (vide supra and Supplementary Figure 9). The self-quenching at high tC^O incorporation affects the relative brightness of the transcripts such that maximum emission is achieved at 75% (Supplementary Figure 9). Importantly, due to the minor differences in incorporation preference between tC^OTP and CTP, we show that it is possible to tune, with accuracy, the labeling density of mRNA to optimize the relationship between brightness and biological function (for example in translation as discussed below).

In vitro translation of tC^O-labeled mRNA. We next demonstrated that tC^O-labeled mRNA is functional in translation, providing the first evidence that this is possible using an FBA-modified mRNA. We used a commercial transcription-translation kit to produce Calmodulin-3 under cell-free conditions in bacterial lysates (Figure 1, yellow arrows). mRNA, with the same tC^OTP/CTP ratios as used above (0 to 100% of tC^OTP), was produced using the Calmodulin-3 DNA template plasmid provided with the kit, i.e. without any codon optimization. The expression of Calmodulin-3 protein was confirmed by SDS PAGE followed by Coomassie staining (Figure 5a) as well as Western Blot (Figure 5b). Densiometric analysis of the gel bands suggests that protein production from tC^O is comparable to that of non-labeled control (80%–137%; one-way Anova analysis with Tukey's post-hoc test showed that the observed differences in means were not significant; i.e. tC^O content had no effect on the degree of translation; $p<0.05$) (Figure 5c). This demonstrates, importantly, that tC^O, unlike other sugar-[52] or base-modified[59] nucleotide analogues, does not impair ribosomal processing and thereby enables protein translation in cell-free systems. tC^O therefore functions as a novel fluorescent mimic of cytosine in both transcription and translation.

Translation and visualization of tC^O-labeled mRNA in human cells. Having reported that tC^O-labeled mRNAs can be translated by bacterial ribosomal machineries in vitro, we progressed to test their functionality in human cells. The cell-free transcribed H2B:GFP-encoding mRNAs with different tC^O-content were introduced into SH-SY5Y neuroblastoma by both electroporation and chemical transfection; the latter mimicking drug delivery (Figure 1, second green arrow). The transcripts used were 5'-capped and 3'-protected by poly-adenylation (by ca. 300 nt). This was necessary to diminish mRNA degradation for the natural as well as tC^O-containing mRNA, and the results suggested neither negative nor positive effects of this FBA on cellular mRNA stability.

We show by confocal fluorescence microscopy imaging of live human cells that tC^O-labeled mRNAs are accurately translated resulting in the expression of a correctly localized (nuclear) and folded (fluorescent) protein product (Figure 6a and 6c, Supplementary Figure 10a and b). This is the first published observation that an FBA-modified mRNA can be functional in cells and efficiently processed by human ribosomal machineries. Furthermore, this finding supports our reported low frequency of

misincorporations of tC^O into RNA during cell-free transcription.

We thereafter used flow cytometry to quantify the translation of protein, based on GFP fluorescence following electroporation (Figure 6a and 6b) or chemical transfection (Figure 6c) at three time points post-transfection. Electroporation was used to introduce mRNA directly to the cytosol and based on transfection efficiency (i.e. number of GFP-positive cells) this, highly invasive, method was more effective than chemical transfection using lipofectamine (Supplementary Figure 10c). However, we also observed that the

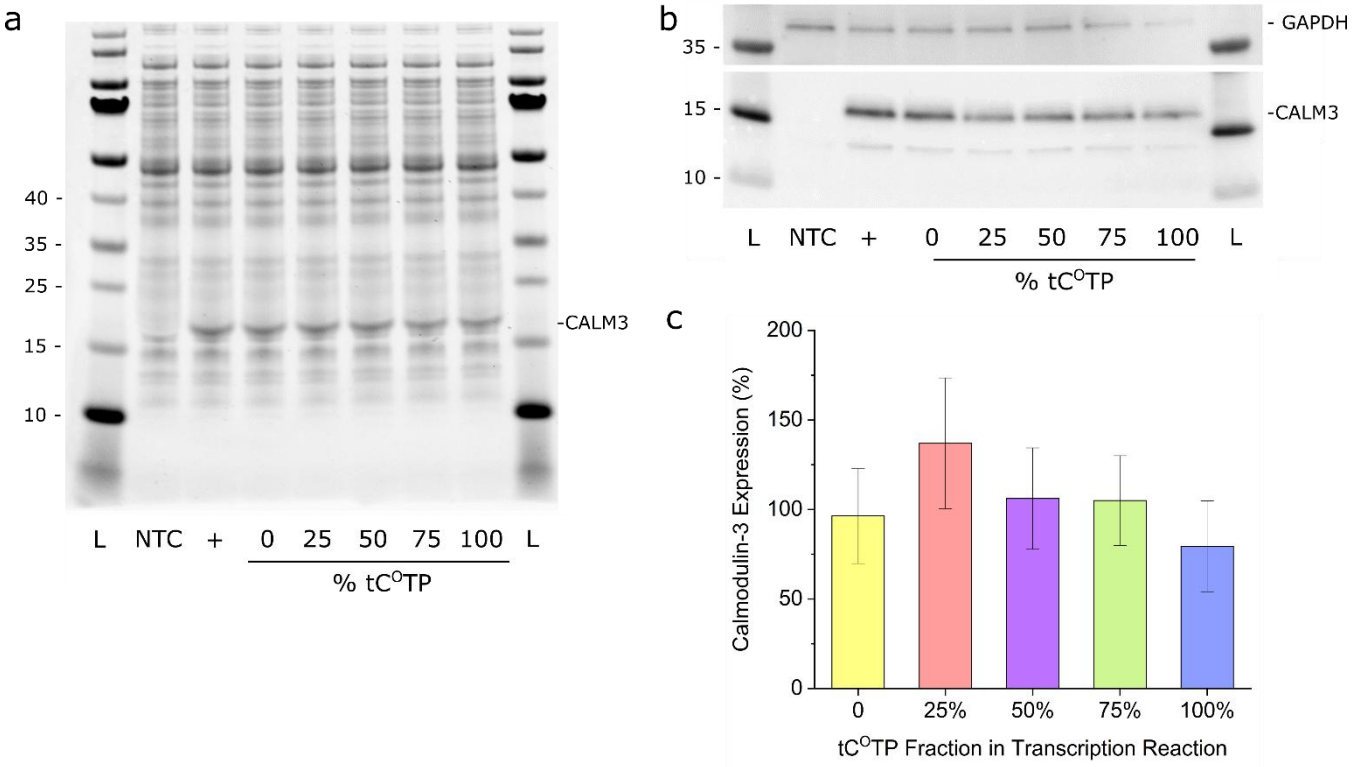

Figure 5. **Cell-free translation of Calmodulin-3 (CALM3) mRNA.** a) Coomassie staining and b) Western Blot (WB) of the in vitro translation reactions. NTC: no template control; +: kit template RNA control. The PageRuler Prestained Protein Ladder was used. c) Quantification by WB and densitometry analysis (mean % of control ± standard deviation; n=3). One-way ANOVA with means comparison using Tukey's post-hoc test showed no significant effect of tC^O content in the mRNA transcripts on protein translation ($p<0.05$).

transfection efficiency following electroporation decreased linearly with increasing tC^O content; an effect that rendered an effective lowering of the mean fluorescence intensity of the cell populations electroporated with mRNA containing tC^O. The reasons for this effect are unclear, but it is possible that the electric field used caused some tC^O mRNA degradation and/or imposed secondary structures that prevented translation. In any case, the effect was not associated with toxicity (Supplementary Figure 10g) and the fluorescence signal persisted over 72 h post-electroporation. During this time the GFP fluorescence gradually decreased in all samples (Figure 6a). This is likely a combined effect of cell division (the doubling time of SH-SY5Y cells under our experimental conditions is approximately 24 hours) and cytosolic mRNA degradation; none of these effects appear affected by tC^O-content, suggesting that the tC^O-labeled mRNA that reach the cytosol in a functional form is behaving as the corresponding non-labeled mRNA.

Chemical transfection resulted in considerably fewer GFP-positive cells (Supplementary Figure 10c) but, importantly, no tC^O-dependent effects on either transfection efficiency or mean cellular GFP fluorescence were observed (Figure 6b). This is in agreement with the cell-free translation experiments (Figure 5) and suggests that tC^O-labeled mRNA, if appropriately delivered, is processed as effectively as non-labeled mRNA by human ribosomes (see Figure 6f and further below). In this case, the mean fluorescence intensity increases over time (Figure 6b). This reflects a continuous lipofectamine-mediated and tC^O-independent endocytic uptake and escape of mRNA cargo to the cytosol lasting for several days, again emphasizing that this FBA has cytosine-mimicking properties that affects neither lipid complexation nor endosomal escape processes of mRNA during cellular delivery.

Importantly, the complexation of the tC^O-labeled mRNA with lipofectamine enabled its direct visualization inside cells using live cell confocal microscopy (Figure 6c, red puncta). This represents the first observation of FBA-labeled nucleic acids inside of a living cell and demonstrates that tC^O is bright enough to be tracked following 405 nm excitation and yielded sufficient contrast over the autofluorescent cellular background that is typical to live cells. We therefore proceeded to visualize, in real time, both the uptake and subsequent translation of an FBA-modified mRNA by time-lapse recordings of cells over-

expressing an early endosome biomarker (mRFP-Rab5) (Figure 6d). We observed co-localization of the tC^O signal with mRFP-Rab5 proteins, highlighting the fact that the mRNA transits through the early endosome following endocytosis (Figure 6d and Supplementary Movie 1). Importantly, our results show a successful new methodology that enables not only simultaneous spatiotemporal tracking of the uptake and trafficking of mRNA during cellular delivery and the appearance of its correctly localized and folded translation product but also reports on the natural, unperturbed expression level of this delivered mRNA.

Finally, we compared the in-cell translation efficiency of the tC^O-labeled mRNA to that of a commercial GFP-encoding Cy5 backbone-labeled variant (with ca. 25% of all U positions carrying the Cy5 dye) (Figure 6e). Despite the

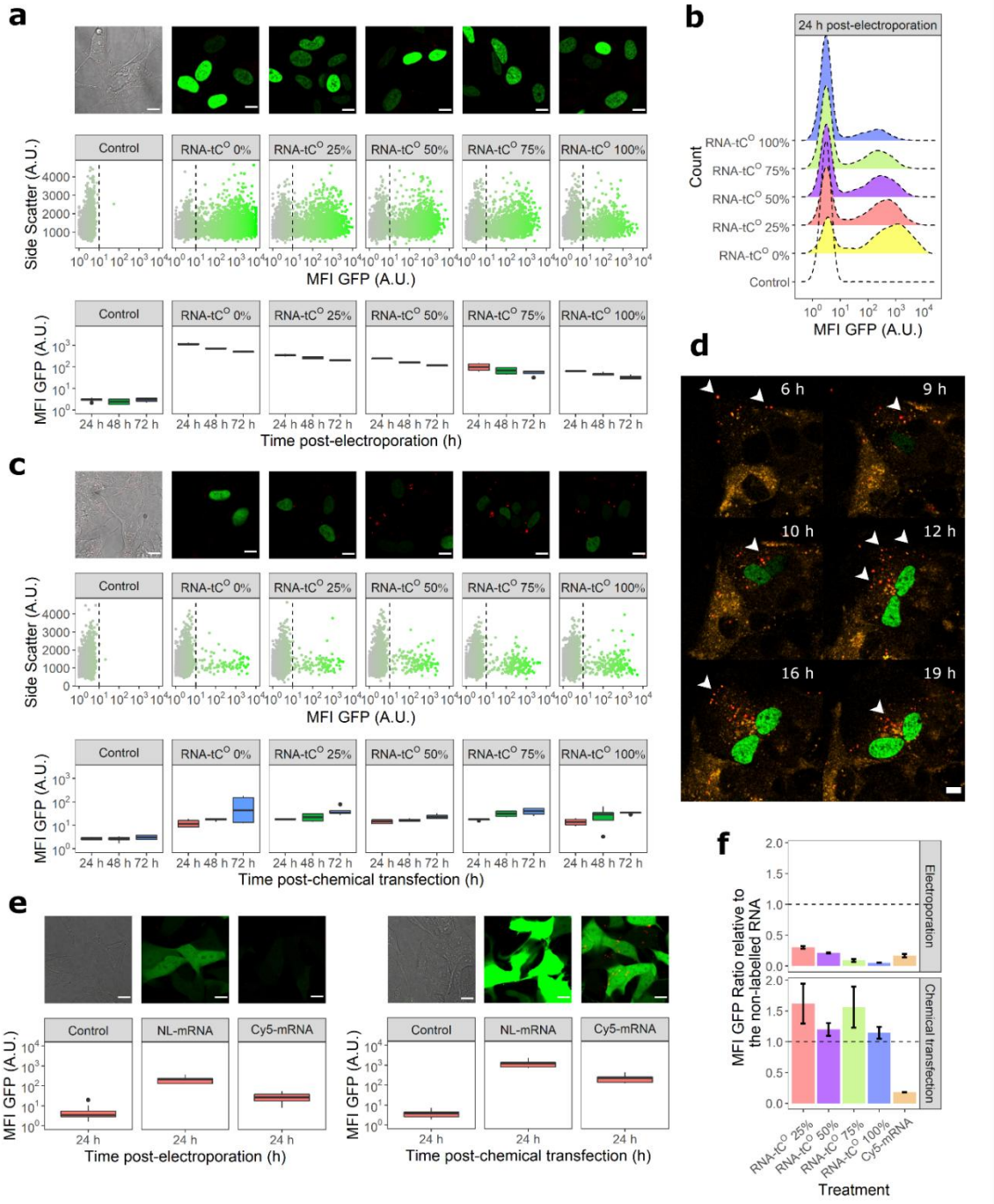

Figure 6. Translation and visualization of tC^O-labeled mRNA in human SH-SY5Y cells. The mRNA translation was monitored based on the fluorescence intensity of the encoded H2B:GFP protein using confocal microscopy and flow cytometry. (a) mRNA translation following electroporation; (top) confocal images (3x enlargements, scale bars: 10 μm) recorded 24 h post-electroporation, (middle) flow cytometry scatter plots 24 h post-electroporation, and (bottom) mean cellular GFP fluorescence intensity (MFI GFP± standard deviation) of all counted cells at 24, 48, and 72 h post-electroporation. (b) Representative MFI GFP histograms corre-

sponding to the distributions in (a). (c) mRNA translation following chemical transfection (lipofection), corresponding to the data shown in (a). (top) confocal images (3x enlargements, scale bars: 10 μm) recorded 48 h post-chemical transfection, (middle) flow cytometry scatter plots 48 h post-electroporation, and (bottom) MFI GFP of all counted cells at 24, 48, and 72 h post-chemical transfection (d) Cells overexpressing mRFP-Rab5 (early endosome biomarker) were chemically transfected with 75% tC^O-labeled mRNA and followed overtime to validate tC^O as an intracellular mRNA tracking probe (white arrows), scale bars: 10 μm. (e) mRNA translation of Cyanine5-labeled (Cy5) eGFP encoding mRNAs (TriLink®) 24 h post-transfection (electroporation or chemical transfection). NL; non-labeled. Scale bars: 10 μm. (f) The impact of tC^O or Cy5 incorporation on mRNA translation, represented as the ratio of cellular MFI GFP of the labeled mRNA relative to the cellular MFI GFP for the corresponding non-labeled RNA. All cell experiments were performed in three biological replicates.

low labeling density, the Cy5-labeled mRNA has only ca. 20% of the translation capacity of corresponding GFP-encoding nonlabeled mRNA following both electroporation and chemical transfection (Figure 6f). This is consistent with previous in vitro translation studies that confirm the translation-impeding nature of the Cy5 modification.[8] The most noticeable finding of this comparison is that lipofectamine-delivered tC^O-labeled mRNAs, in contrast to the Cy5-labeled variant, promote virtually similar H2B:GFP translation compared to the corresponding non-labeled mRNA (Figure 6f). This confirms the above conclusion that tC^O does not impair the ability of mRNA to be processed by human ribosomes if appropriately presented. This is possibly due to the absence of fluorophore charge and negligible steric hindrance in the tC^O-labeled RNA. In contrast, Cy5, currently the most common commercial fluorophore for mRNA labeling, has a significant amphiphilic character and is attached to UTP via a linker overall adding considerable bulkiness, which altogether may impede its processing by ribosomes.

CONCLUSION

In this study we demonstrate that tC^O, a fluorescent cytosine base analogue with moderate chemical modification, in a remarkable way takes the role of natural cytosine in a number of biochemical processes. This FBA, is correctly recognized by several enzymatic machineries, including RNA polymerases, reverse transcriptase and bacterial as well as human ribosomes. We have also developed a robust, generic, and affordable synthesis method to produce the triphosphate variants of unnatural nucleotides, presenting the first successful synthesis of the tC^O nucleotide. This chemical development is critical to enable the use of tC^O and other FBAs in biochemical and biological applications.

We demonstrate that tC^O can be incorporated into RNA of any length via both end-labeling and cell-free transcription, which enables versatile introduction of FBAs in both flanking and functional segments of different kinds of RNA. Importantly, we have managed to incorporate tC^O in up to 100% of natural cytosine positions of a full-length 1.2 kb mRNA, without any premature abortions. Analysis of the transcription products demonstrated that tC^O is incorporated into RNA virtually as efficiently as native CTP and therefore constitutes a true nature-mimicking fluorescent modification in this respect.

Astoundingly, we also found that tC^O-labeled mRNA is correctly translated, both in vitro and in live cells, yielding correctly folded and localized protein products. This has never previously been shown for FBA-modified mRNA; in fact previous published work using the cytosine-analogue tC failed to generate translation competent mRNA even starting from a considerably shorter (0.8 kB) template. Intriguingly, the translation efficiency of our mRNAs is independent of tC^O content as opposed to the performance of commercial Cy5-labeled mRNA which is only moderately tolerated by ribosomes even if the labeling density is low. This points to the flexibility and versatility of the herein discovered tC^O-labeling method, which offers opportunity to tune labeling density to optimize brightness and distribution of fluorophores along the mRNA sequence. Moreover, when using Cy5-labeled mRNA to study delivery the modus in the field is to mix in a fraction of the labeled mRNA with the corresponding unlabeled mRNA, a procedure that increases the risk of incorrectly reported rates and levels of delivery and translation even further; something that now can be avoided with our nature-mimicking labeling technique.

Finally, we present the first example of that an FBA-labeled nucleic acid can be directly visualized in live cells, showing that tC^O's brightness and absorption at 405 nm is sufficient to overcome previous limitations with FBA probes in biological applications.[30] Moreover, we demonstrate how this conveniently allows for spatiotemporal monitoring of mRNA uptake, trafficking and organelle colocalization in a live cell model with simultaneous detection of its unperturbed translation into H2B:GFP protein, expressed at natural levels, in live-cell confocal microscopy using selective excitation.

We envision that our straightforward approach for introducing non-perturbing fluorescent labels into RNA will be an excellent addition to existing imaging tools, applicable for elucidating trafficking mechanisms such as endosomal escape and exosome formation, both of which are of fundamental importance for pharmaceutical development. Applying both TdT end-labeling and T7 transcription strategies also holds significant combined potential as it would enable selective and site-specific incorporation of dual labels to allow for e.g. FRET applications. We are convinced that the development reported here will benefit pharmaceutical industry, clinical laboratories, and academic partners aiming at furthering their understanding of uptake and endosomal escape mechanisms and allow them to take vital steps towards new and improved delivery strategies for next-generation nucleic acid-based drugs as well as mRNA-based vaccines.

ASSOCIATED CONTENT

Supporting Information. Characterization of tC^OTP, all experimental procedures, sequence alignments, additional electrophoresis gels, confocal images and flow cytometry data are supplied as Supporting Information. Supporting Movie 1 shows the internalization of the 75% tC^O-labeled mRNA and its expression over 55h in Huh7 cells (1 s = 1.1 h). This mate-

rial is available free of charge via the Internet at http://pubs.acs.org.

AUTHOR INFORMATION

Corresponding Authors

*L. Marcus Wilhelmsson email address: marcus.wilhelmsson@chalmers.se.
*Elin K. Esbjörner email address: eline@chalmers.se.

Present Addresses

† Oligonucleotide Discovery, Discovery Sciences, R&D, AstraZeneca, Gothenburg, Sweden.
ǂ Advanced Drug Delivery, Pharmaceutical Sciences, R&D, AstraZeneca, Gothenburg, Sweden.

Author Contributions

The manuscript was written through contributions of all authors. All authors have given approval to the final version of the manuscript.

Notes

A.G., A.D. and T.B. are employees of AstraZeneca and may hold shares in the company.

ACKNOWLEDGMENT

We gratefully acknowledge Prof. Tom Brown at the University of Oxford for fruitful discussions about the triphosphate synthesis and Linda Thunberg at AstraZeneca Gothenburg for help with purification of the triphosphate. This work was conducted as part of the FoRmulaEx research center for nucleotide delivery and with associated financial support to E.K.E. and L.M.W. from the Swedish Foundation for Strategic Research (SSF, grant No. IRC15-0065). F. L.-A., I. S. and M. H. acknowledge funding from Institut Pasteur.

REFERENCES

1. Crooke, S. T.; Witztum, J. L.; Bennett, C. F.; Baker, B. F., RNA-Targeted Therapeutics. *Cell Metabolism* **2018,** *27* (4), 714-739.
2. Dowdy, S. F., Overcoming cellular barriers for RNA therapeutics. *Nat. Biotechnol.* **2017,** *35* (3), 222-229.
3. Crooke, S. T.; Wang, S.; Vickers, T. A.; Shen, W.; Liang, X.-h., Cellular uptake and trafficking of antisense oligonucleotides. *Nat. Biotechnol.* **2017,** *35*, 230.
4. Pei, D.; Buyanova, M., Overcoming Endosomal Entrapment in Drug Delivery. *Bioconjugate Chem.* **2018**.
5. Gilleron, J.; Querbes, W.; Zeigerer, A.; Borodovsky, A.; Marsico, G.; Schubert, U.; Manygoats, K.; Seifert, S.; Andree, C.; Stöter, M.; Epstein-Barash, H.; Zhang, L.; Koteliansky, V.; Fitzgerald, K.; Fava, E.; Bickle, M.; Kalaidzidis, Y.; Akinc, A.; Maier, M.; Zerial, M., Image-based analysis of lipid nanoparticle–mediated siRNA delivery, intracellular trafficking and endosomal escape. *Nat. Biotechnol.* **2013,** *31* (7), 638-646.
6. Armitage, B. A., Cyanine Dye–Nucleic Acid Interactions. In *Heterocyclic Polymethine Dyes: Synthesis, Properties and Applications*, Strekowski, L., Ed. Springer Berlin Heidelberg: Berlin, 2008; pp 11-29.
7. Zhang, Y.; Kleiner, R. E., A Metabolic Engineering Approach to Incorporate Modified Pyrimidine Nucleosides into Cellular RNA. *J. Am. Chem. Soc.* **2019,** *141*, 3347-3351.
8. Custer, T. C.; Walter, N. G., In vitro labeling strategies for in cellulo fluorescence microscopy of single ribonucleoprotein machines. *Protein. Sci.* **2017,** *26* (7), 1363-1379.
9. Shimomura, O.; Johnson, F. H.; Saiga, Y., Extraction, Purification and Properties of Aequorin, a Bioluminescent Protein from the Luminous Hydromedusan, Aequorea. *J. Cell. Compar. Physl.* **1962,** *59* (3), 223-239.
10. Jung, G., Fluorescent Proteins: The Show Must go on! In *Fluorescent Analogues of Biomolecular Building Blocks: Design and Applications*, Wilhelmsson, L. M.; Tor, Y., Eds. Wiley: 2016; pp 55-90.
11. Wittrup, A.; Ai, A.; Liu, X.; Hamar, P.; Trifonova, R.; Charisse, K.; Manoharan, M.; Kirchhausen, T.; Lieberman, J., Visualizing lipid-formulated siRNA release from endosomes and target gene knockdown. *Nat. Biotechnol.* **2015,** *33* (8), 870-6.
12. Li, Y.; Ke, K.; Spitale, R. C., Biochemical Methods To Image and Analyze RNA Localization: From One to Many. *Biochemistry* **2019,** *58* (5), 379-386.
13. Burke, K. S.; Antilla, K. A.; Tirrell, D. A., A Fluorescence in Situ Hybridization Method To Quantify mRNA Translation by Visualizing Ribosome–mRNA Interactions in Single Cells. *ACS Cent. Sci.* **2017,** *3* (5), 425-433.
14. Wadsworth, G. M.; Parikh, R. Y.; Kim, H. D.; Choy, J. S., mRNA detection in budding yeast with single fluorophores. *Nucleic Acids Res.* **2017,** *45* (15), e141-e141.
15. Gaspar, I.; Hövelmann, F.; Chamiolo, J.; Ephrussi, A.; Seitz, O., Quantitative mRNA Imaging with Dual Channel qFIT Probes to Monitor Distribution and Degree of Hybridization. *ACS Chem. Biol.* **2018,** *13* (3), 742-749.
16. He, L.; Lu, D.-Q.; Liang, H.; Xie, S.; Luo, C.; Hu, M.; Xu, L.; Zhang, X.; Tan, W., Fluorescence Resonance Energy Transfer-Based DNA Tetrahedron Nanotweezer for Highly Reliable Detection of Tumor-Related mRNA in Living Cells. *ACS Nano* **2017,** *11* (4), 4060-4066.
17. Wang, B.; Chen, Z.; Ren, D.; You, Z., A novel dual energy transfer probe for intracellular mRNA detection with high robustness and specificity. *Sensor. Actuat. B-Chem.* **2019,** *279*, 342-350.
18. Chen, X.; Zhang, D.; Su, N.; Bao, B.; Xie, X.; Zuo, F.; Yang, L.; Wang, H.; Jiang, L.; Lin, Q.; Fang, M.; Li, N.; Hua, X.; Chen, Z.; Bao, C.; Xu, J.; Du, W.; Zhang, L.; Zhao, Y.; Zhu, L.; Loscalzo, J.; Yang, Y., Visualizing RNA dynamics in live cells with bright and stable fluorescent RNAs. *Nat. Biotechnol.* **2019,** *37* (11), 1287-1293.
19. Urbanek, M. O.; Galka-Marciniak, P.; Olejniczak, M.; Krzyzosiak, W. J., RNA imaging in living cells - methods and applications. *RNA Biol* **2014,** *11* (8), 1083-1095.
20. Bertrand, E.; Chartrand, P.; Schaefer, M.; Shenoy, S. M.; Singer, R. H.; Long, R. M., Localization of ASH1 mRNA Particles in Living Yeast. *Molecular Cell* **1998,** *2* (4), 437-445.
21. Yan, X.; Hoek, T. A.; Vale, R. D.; Tanenbaum, M. E., Dynamics of Translation of Single mRNA Molecules In Vivo. *Cell* **2016,** *165* (4), 976-989.
22. Wang, C.; Han, B.; Zhou, R.; Zhuang, X., Real-Time Imaging of Translation on Single mRNA Transcripts in Live Cells. *Cell* **2016,** *165* (4), 990-1001.
23. Mamot, A.; Sikorski, P. J.; Warminski, M.; Kowalska, J.; Jemielity, J., Azido-Functionalized 5′ Cap Analogues for the Preparation of Translationally Active mRNAs Suitable for Fluorescent Labeling in Living Cells. *Angew. Chem. Int. Ed.* **2017,** *56* (49), 15628-15632.
24. Anhäuser, L.; Hüwel, S.; Zobel, T.; Rentmeister, A., Multiple covalent fluorescence labeling of eukaryotic mRNA at the poly(A) tail enhances translation and can be performed in living cells. *Nucleic Acids Res.* **2019,** *47* (7), e42-e42.
25. Croce, S.; Serdjukow, S.; Carell, T.; Frischmuth, T., Chemoenzymatic Preparation of Functional Click-Labeled Messenger RNA. *ChemBioChem* **2020,** *21* (11), 1641-1646.
26. Ziemniak, M.; Szabelski, M.; Lukaszewicz, M.; Nowicka, A.; Darzynkiewicz, E.; Rhoads, R. E.; Wieczorek, Z.; Jemielity, J.,

Synthesis and evaluation of fluorescent cap analogues for mRNA labelling. *RSC advances* **2013,** *3* (43), 20943-20958.

27. Xu, W.; Chan, K. M.; Kool, E. T., Fluorescent nucleobases as tools for studying DNA and RNA. *Nat. Chem.* **2017,** *9*, 1043.

28. Sinkeldam, R. W.; Greco, N. J.; Tor, Y., Fluorescent Analogs of Biomolecular Building Blocks: Design, Properties, and Applications. *Chem. Rev.* **2010,** *110* (5), 2579-2619.

29. Wilhelmsson, L. M., Fluorescent nucleic acid base analogues. *Q. Rev. Biophys.* **2010,** *43* (2), 159-183.

30. Xu, W.; Chan, K. M.; Kool, E. T., Fluorescent nucleobases as tools for studying DNA and RNA. *Nat. Chem.* **2017,** *9* (11), 1043-1055.

31. Börjesson, K.; Preus, S.; El-Sagheer, A. H.; Brown, T.; Albinsson, B.; Wilhelmsson, L. M., Nucleic Acid Base Analog FRET-Pair Facilitating Detailed Structural Measurements in Nucleic Acid Containing Systems. *J. Am. Chem. Soc.* **2009,** *131* (12), 4288-4293.

32. Füchtbauer, A. F.; Preus, S.; Börjesson, K.; McPhee, S. A.; Lilley, D. M. J.; Wilhelmsson, L. M., Fluorescent RNA cytosine analogue – an internal probe for detailed structure and dynamics investigations. *Sci. Rep.* **2017,** *7* (1), 2393.

33. Füchtbauer, A. F.; Wranne, M. S.; Bood, M.; Weis, E.; Pfeiffer, P.; Nilsson, J. R.; Dahlén, A.; Grøtli, M.; Wilhelmsson, L. M., Interbase FRET in RNA: from A to Z. *Nucleic Acids Res.* **2019,** *47* (19), 9990-9997.

34. Liu, W.; Shin, D.; Ng, M.; Sanbonmatsu, K. Y.; Tor, Y.; Cooperman, B. S., Stringent Nucleotide Recognition by the Ribosome at the Middle Codon Position. *Molecules (Basel, Switzerland)* **2017,** *22* (9), 1427.

35. Stengel, G.; Urban, M.; Purse, B. W.; Kuchta, R. D., Incorporation of the Fluorescent Ribonucleotide Analogue tCTP by T7 RNA Polymerase. *Anal. Chem.* **2010,** *82* (3), 1082-1089.

36. McCoy, L. S.; Shin, D.; Tor, Y., Isomorphic Emissive GTP Surrogate Facilitates Initiation and Elongation of in Vitro Transcription Reactions. *J. Am. Chem. Soc.* **2014,** *136* (43), 15176-15184.

37. Li, Y.; Fin, A.; McCoy, L.; Tor, Y., Polymerase-Mediated Site-Specific Incorporation of a Synthetic Fluorescent Isomorphic G Surrogate into RNA. *Angew. Chem. Int. Ed.* **2017,** *56* (5), 1303-1307.

38. Tanpure, A. A.; Srivatsan, S. G., A Microenvironment-Sensitive Fluorescent Pyrimidine Ribonucleoside Analogue: Synthesis, Enzymatic Incorporation, and Fluorescence Detection of a DNA Abasic Site. *Chem. Eur. J.* **2011,** *17* (45), 12820-12827.

39. Manna, S.; Srivatsan, S. G., Synthesis and Enzymatic Incorporation of a Responsive Ribonucleoside Probe That Enables Quantitative Detection of Metallo-Base Pairs. *Org. Lett.* **2019,** *21* (12), 4646-4650.

40. Yoshikawa, M.; Kato, T.; Takenishi, T., Studies of Phosphorylation. III. Selective Phosphorylation of Unprotected Nucleosides. *Bulletin of the Chemical Society of Japan* **1969,** *42* (12), 3505-3508.

41. Ludwig, J.; Eckstein, F., Rapid and efficient synthesis of nucleoside 5'-0-(1-thiotriphosphates), 5'-triphosphates and 2',3'-cyclophosphorothioates using 2-chloro-4H-1,3,2-benzodioxaphosphorin-4-one. *J. Org. Chem.* **1989,** *54* (3), 631-635.

42. Roy, B.; Depaix, A.; Périgaud, C.; Peyrottes, S., Recent Trends in Nucleotide Synthesis. *Chem. Rev.* **2016,** *116* (14), 7854-7897.

43. Burgess, K.; Cook, D., Syntheses of Nucleoside Triphosphates. *Chem. Rev.* **2000,** *100* (6), 2047-2060.

44. Flamme, M.; McKenzie, L. K.; Sarac, I.; Hollenstein, M., Chemical methods for the modification of RNA. *Methods* **2019,** *161*, 64-82.

45. Hocek, M., Enzymatic Synthesis of Base-Functionalized Nucleic Acids for Sensing, Cross-linking, and Modulation of Protein–DNA Binding and Transcription. *Accounts Chem. Res.* **2019,** *52* (6), 1730-1737.

46. Sarac, I.; Meier, C., Efficient Automated Solid-Phase Synthesis of DNA and RNA 5′-Triphosphates. *Chem. Eur. J.* **2015,** *21* (46), 16421-16426.

47. Gaur, R. K.; Sproat, B. S.; Krupp, G., Novel solid phase synthesis of 2'-o-methylribonucleoside 5'-triphosphates and their α-thio analogues. *Tet. Lett.* **1992,** *33* (23), 3301-3304.

48. Sarac, I.; Hollenstein, M., Terminal Deoxynucleotidyl Transferase in the Synthesis and Modification of Nucleic Acids. *ChemBioChem* **2019,** *20* (7), 860-871.

49. Motea, E. A.; Berdis, A. J., Terminal deoxynucleotidyl transferase: The story of a misguided DNA polymerase. *Biochimica et Biophysica Acta (BBA) - Proteins and Proteomics* **2010,** *1804* (5), 1151-1166.

50. Srivatsan, S. G.; Tor, Y., Fluorescent Pyrimidine Ribonucleotide: Synthesis, Enzymatic Incorporation, and Utilization. *J. Am. Chem. Soc.* **2007,** *129* (7), 2044-2053.

51. Vaught, J. D.; Dewey, T.; Eaton, B. E., T7 RNA Polymerase Transcription with 5-Position Modified UTP Derivatives. *J. Am. Chem. Soc.* **2004,** *126* (36), 11231-11237.

52. Aurup, H.; Siebert, A.; Benseler, F.; Williams, D.; Eckstein, F., Translation of 2'-modified mRNA in vitro and in vivo. *Nucleic Acids Res.* **1994,** *22* (23), 4963-4968.

53. Smith, C. C.; Hollenstein, M.; Leumann, C. J., The synthesis and application of a diazirine-modified uridine analogue for investigating RNA–protein interactions. *RSC Advances* **2014,** *4* (89), 48228-48235.

54. Domnick, C.; Eggert, F.; Kath-Schorr, S., Site-specific enzymatic introduction of a norbornene modified unnatural base into RNA and application in post-transcriptional labeling. *Chem. Comm.* **2015,** *51* (39), 8253-8256.

55. Temiakov, D.; Patlan, V.; Anikin, M.; McAllister, W. T.; Yokoyama, S.; Vassylyev, D. G., Structural Basis for Substrate Selection by T7 RNA Polymerase. *Cell* **2004,** *116* (3), 381-391.

56. Lakowicz, J. R., Principles of Fluorescence Spectroscopy, 3rd edition. In *Principles of Fluorescence Spectroscopy*, 3rd Edition ed.; Springer: Boston, 2006.

57. Stengel, G.; Urban, M.; Purse, B. W.; Kuchta, R. D., High Density Labeling of Polymerase Chain Reaction Products with the Fluorescent Base Analogue tCo. *Anal. Chem.* **2009,** *81* (21), 9079-9085.

58. Stengel, G.; Purse, B. W.; Wilhelmsson, L. M.; Urban, M.; Kuchta, R. D., Ambivalent Incorporation of the Fluorescent Cytosine Analogues tC and tCo by Human DNA Polymerase α and Klenow Fragment. *Biochemistry* **2009,** *48* (31), 7547-7555.

59. Noyon, C.; Roumeguère, T.; Delporte, C.; Dufour, D.; Cortese, M.; Desmet, J.-M.; Lelubre, C.; Rousseau, A.; Poelvoorde, P.; Nève, J.; Vanhamme, L.; Boudjeltia, K. Z.; Van Antwerpen, P., The presence of modified nucleosides in extracellular fluids leads to the specific incorporation of 5-chlorocytidine into RNA and modulates the transcription and translation. *Mol. Cell. Biochem.* **2017,** *429* (1), 59-71.

SYNOPSIS TOC (Word Style “SN_Synopsis_TOC”). If you are submitting your paper to a journal that requires a synopsis graphic and/or synopsis paragraph, see the Instructions for Authors on the journal’s homepage for a description of what needs to be provided and for the size requirements of the artwork.

Authors are required to submit a graphic entry for the Table of Contents (TOC) that, in conjunction with the manuscript title, should give the reader a representative idea of one of the following: A key structure, reaction, equation, concept, or theorem, etc., that is discussed in the manuscript. Consult the journal’s Instructions for Authors for TOC graphic specifications.

Insert Table of Contents artwork here